CLASSIFICATION OF FAILURE MODES FOR UNCONFINED COMPRESSION TESTS OF MULTI-YEAR RIDGE ICE

BY

J. F. DORRIS

TECHNICAL INFORMATION RECORD

BRC–1285
JULY 1985

Project No. 27802.34
Mechanical Properties of Sea Ice Phase I

SHELL DEVELOPMENT COMPANY
A DIVISION OF SHELL OIL COMPANY
BELLAIRE RESEARCH CENTER
HOUSTON, TEXAS

TABLE OF CONTENTS

LIST OF ILLUSTRATIONS

LIST OF TABLES

TECHNICAL INFORMATION RECORD BRC-1285

CLASSIFICATION OF FAILURE MODES FOR UNCONFINED COMPRESSION TESTS OF MULTI-YEAR RIDGE ICE

BY

J. F. DORRIS

INTRODUCTION

One of the main goals of the Mechanical Properties of Sea Ice (MPSI) program is to develop constitutive relations which describe the stress-strain behavior of multi-year ice. The constitutive relations can then be used in boundary value problems to describe the interaction of an ice feature (e.g., a multi-year ice ridge) and an offshore Arctic structure. To predict the maximum load transmitted to a structure, the constitutive relations must be complemented with failure criteria which describe the ultimate load capacity of the ice feature. As a first step in developing failure criteria for multi-year ice, the failure of uniaxial compression specimens will be considered. In Phase I of MPSI, approximately 230 uniaxial compression tests were conducted at temperatures of -5°C and -20°C and strain rates of 10^{-5}/sec and 10^{-3}/sec. For a large majority of these tests, there are available photographs of the tested specimens. Based on these photographs, a classification scheme has been developed to describe the failure modes observed in the uniaxial compression of multi-year ridge ice.

FUNDAMENTAL FAILURE MODES

The term failure mode usually is used to describe the state of a completely ruptured test specimen. In Phase I, the uniaxial compression test specimens were deformed at a constant strain rate until either the specimen completely ruptured or 5% longitudinal strain was reached. In cases where the test specimen did not rupture, failure mode will refer to the apparent conditions existing in the specimen at the time the test was concluded. These conditions may or may not describe the actual failure mode if deformation had been allowed to continue. There are three fundamental modes of failure observed in the Phase I compression tests:

1. Shear Failure - This failure mode is characterized by a localized deformation along a plane generally oriented at angles greater than 45° with respect to the horizontal direction. Within the shear plane, the material is highly fissured and/or has undergone considerable ductile flow along the shear plane (i.e., the direction of slip). Outside of the shear plane there is little or no deformation. The distorted shape of the test specimen is typically nonsymmetric with two localized bulges at either end of the shear plane. If complete rupture occurs, the test specimen usually fractures along the shear plane into two wedge-shaped pieces.

2. Longitudinal Splitting - This failure mode is characterized by the propagation of large cracks in directions parallel to the longitudinal axis of the test specimen. Other than the opening of these cracks, there is little or no distortion of the test specimen. It is frequently observed that many of the test specimens contain areas of spalling where large slabs of the specimen break away. When complete rupture occurs, the test specimen is usually fractured into several irregularly shaped pieces. In this case it is often observed that the material adhering to the endcaps has a tendency to form a rough cone-like surface.

3. Crushing Failure - The crushing mode is characterized by a symmetric distortion of the test specimen. The distortion may either be a uniform bulging of the entire specimen or a localized bulging. The bulged area of the specimen is highly deformed and usually contains a uniform distribution of microcracks. If localized bulging occurs there is seldom significant deformation or microcracking outside of the bulged area. Specimens failing in the crushing mode rarely rupture completely. If rupture does occur it is usually as a result of the development of a shear plane. This is due largely to the constraint imposed on the material by the endcaps. The endcaps prevent lateral expansion of the ends of the specimen creating shear stresses in the ends. These shear stresses will ultimately cause failure of the test specimen even though a major portion of the material has undergone a relatively homogeneous compressive deformation.

Figures 1-3 are sketches which illustrate the main characteristics of each fundamental failure mode. Figures 4-6 are photographs of typical examples of each principal mode of failure. Depending on the type of lighting used to illuminate each specimen, the zones of extensive microcracking and deformation can easily be determined. If back lighting is used, the zones of

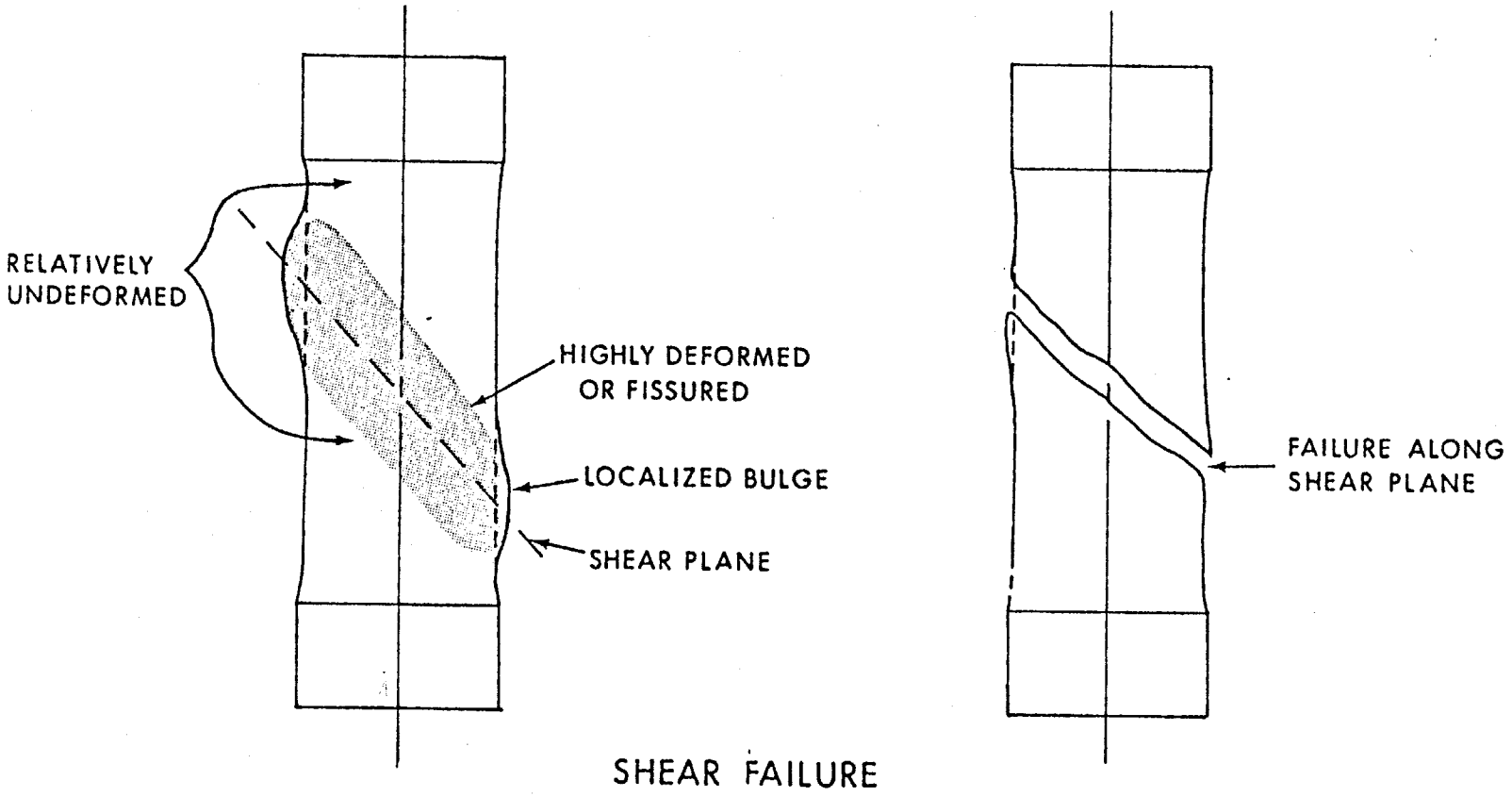

Fig. 1 - Schematic diagram of the fundamental shear failure mode.

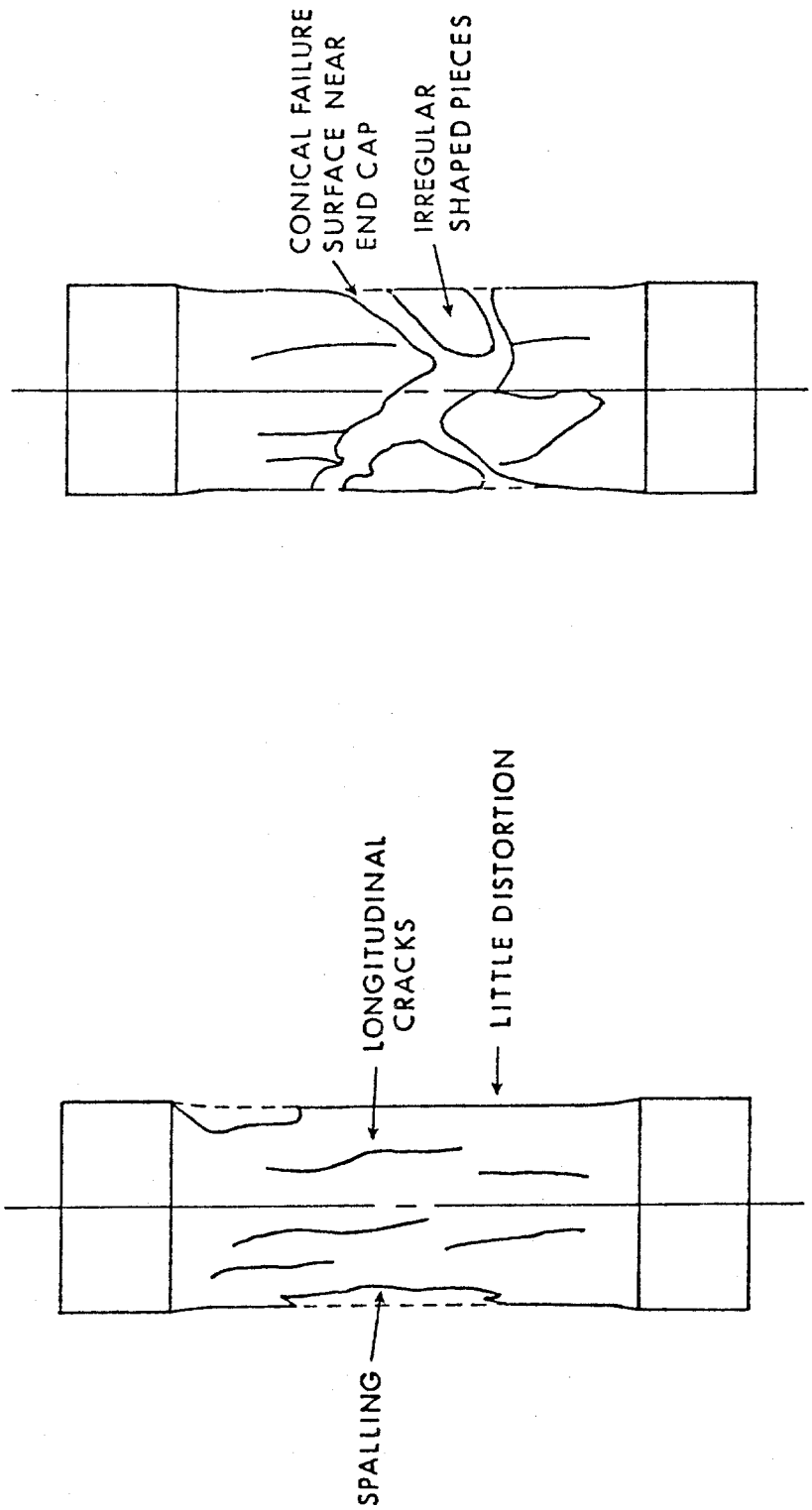

Fig. 2 - Schematic diagram of the fundamental longitudinal splitting failure mode.

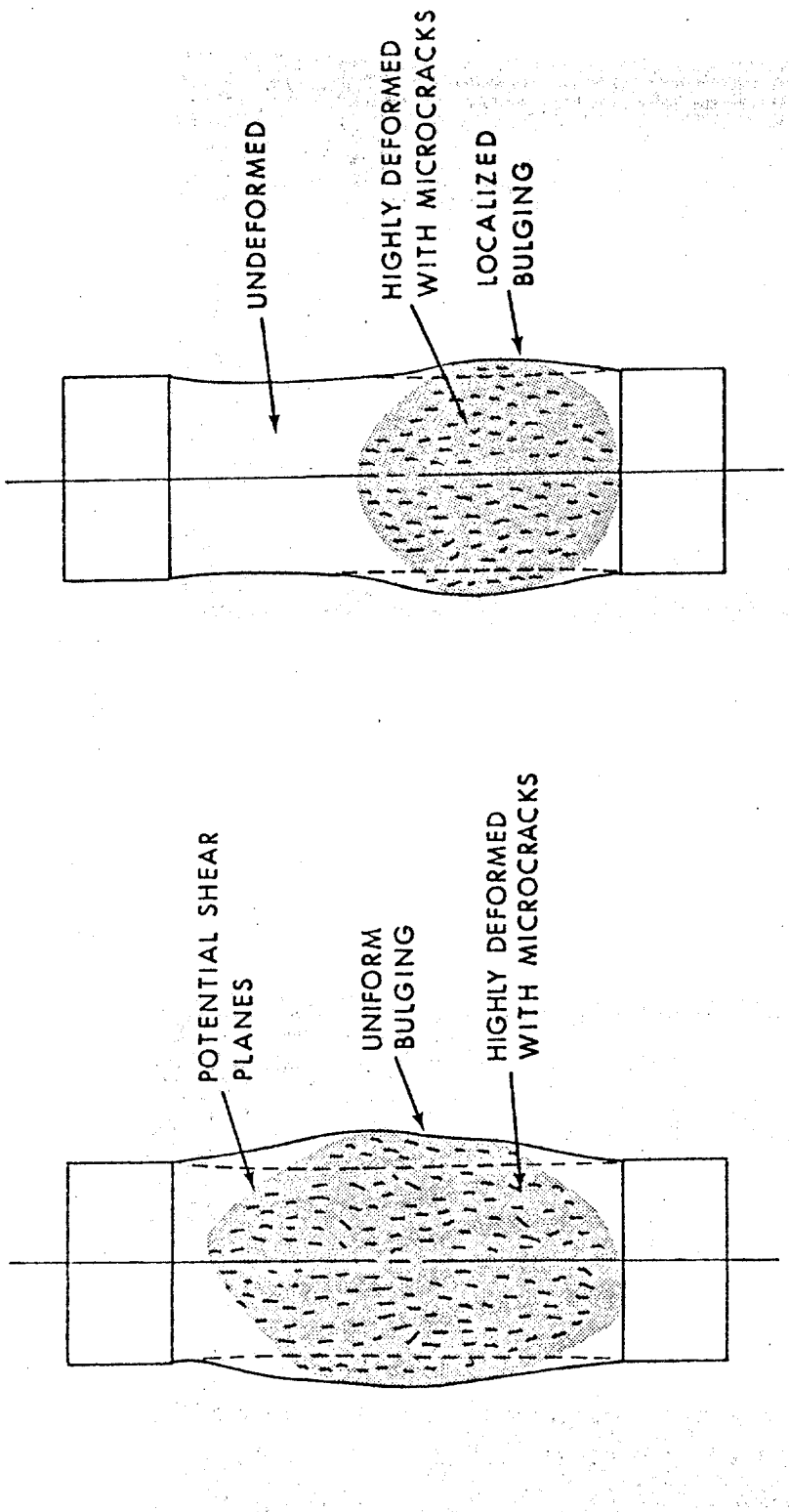

Fig. 3 - Schematic diagram of the fundamental crushing failure mode.

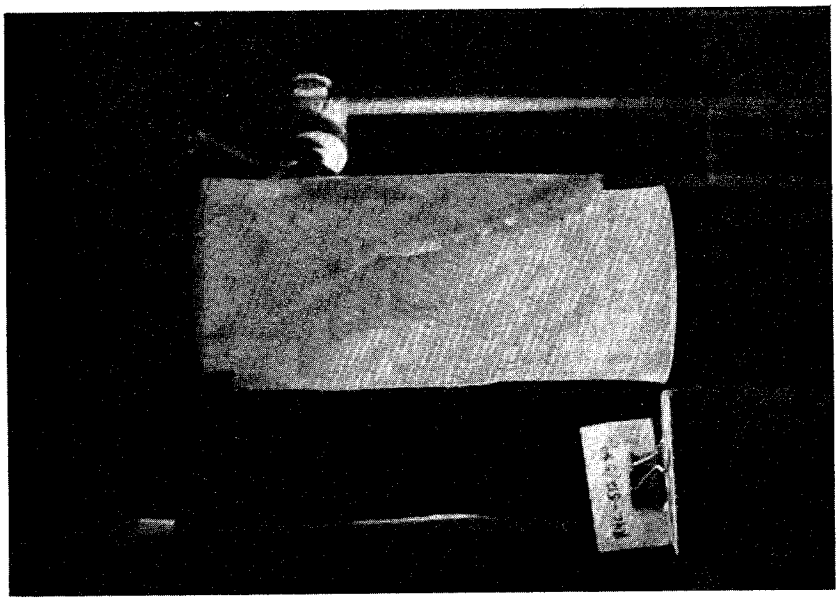

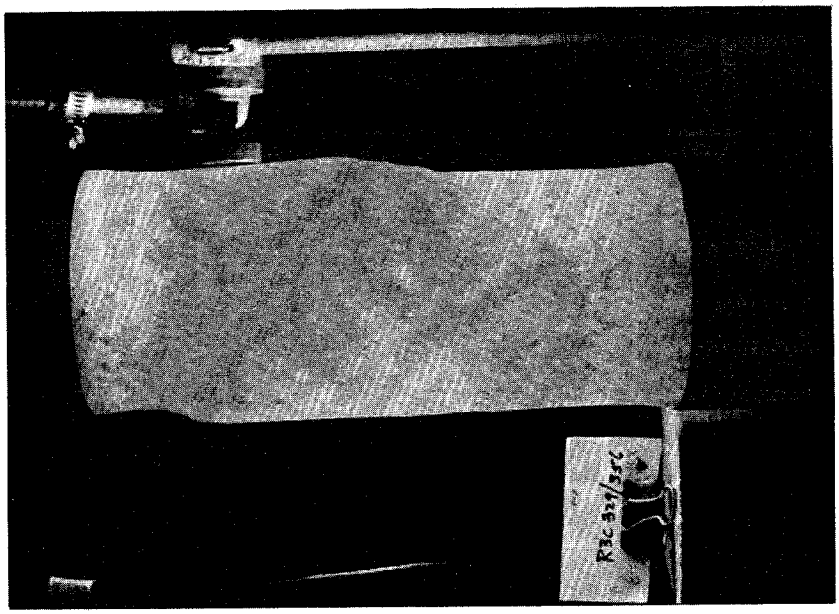

Fig. 4 - Photographic example of the fundamental shear failure mode.

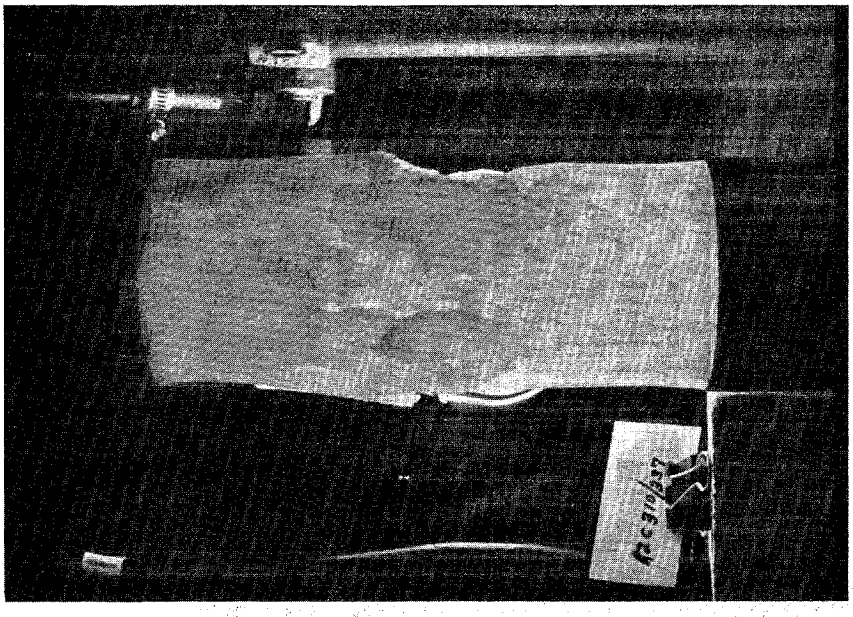

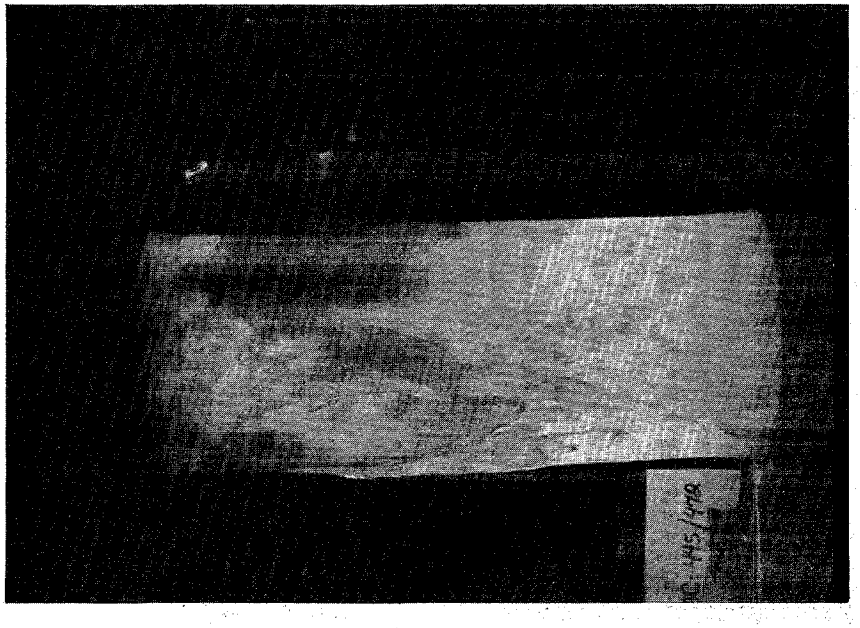

Fig. 5 - Photographic example of the fundamental longitudinal splitting failure mode.

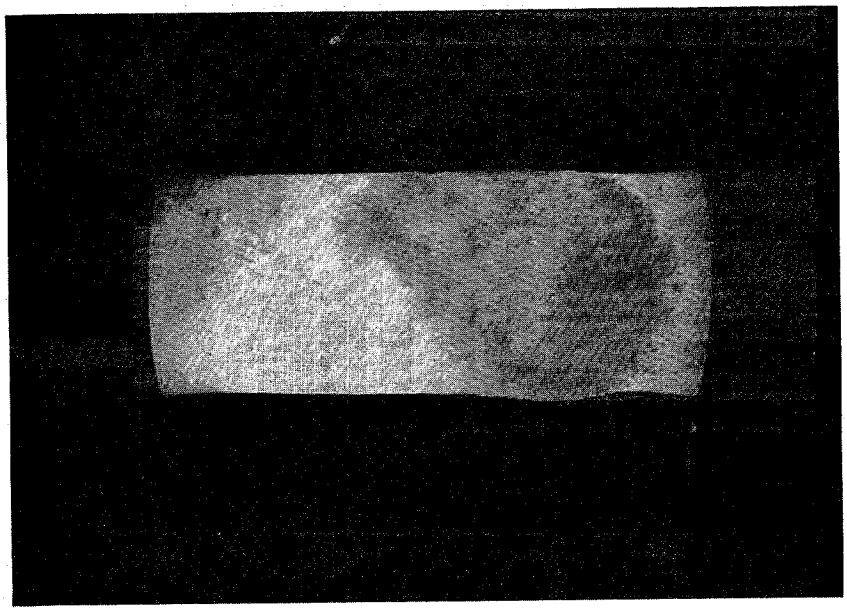

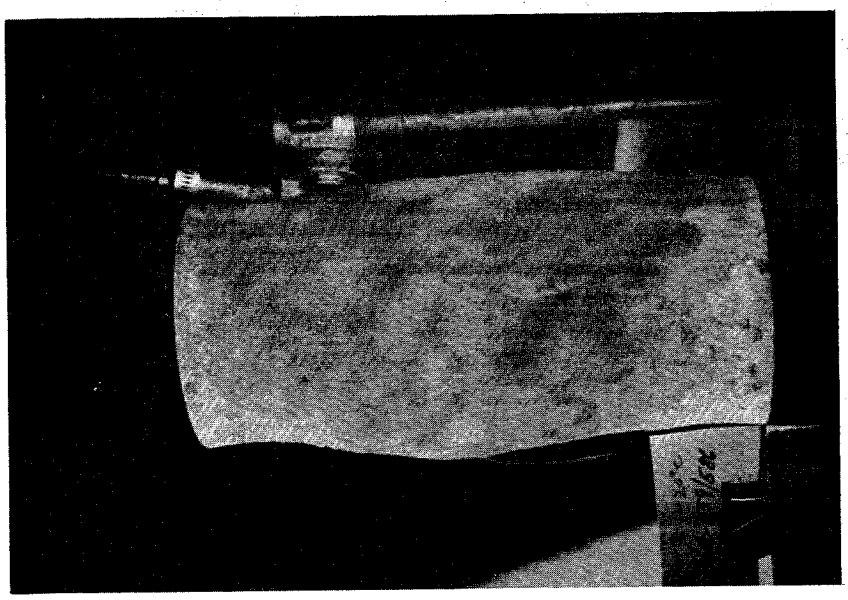

Fig. 6 - Photographic example of the fundamental crushing failure mode.

cracking and deformation appear as darkened areas of the test specimen, whereas in normal room light, the zones appear as lightened areas. All photographs in this report were made with back lighting.

CLASSIFICATION OF FAILURE MODES

Inspection of the photographs of the tested uniaxial specimens reveals that there is very often more than one fundamental failure mode present. As a consequence, a classification scheme has been devised to account for mixed modes of failure. In this scheme, the numbers 1, 2, 3 are assigned to the shear, longitudinal splitting, and crushing modes, respectively. By combining these numbers to form a two digit number, a mixed failure mode is created. The first digit is used to describe the dominant failure mode and the second digit describes a secondary mode of failure. For example, a mixed failure mode labeled 13 would indicate shear as the dominant mode with crushing as the secondary mode. A zero appearing as the second digit indicates that there is no secondary mode.

It is often very difficult to distinguish between the dominant and secondary failure modes. As a general rule the dominant mode is chosen by selecting the mode which appears to have controlled deformation up to the conclusion of the test or the mode which appears to be the apparent cause of rupture. For example, consider the photographs in Figure 7. In both photographs there are clearly nonsymmetric bulges which, if joined by a line, would trace out an apparent shear plane. There can also be seen evidence of crushing by noting the darkened areas above the shear plane. However, in both cases, due to the presence of the bulges, it appears that the endcaps have been displaced laterally with respect to each other indicating slip along the shear plane to be the controlling deformation. Hence these photographs are labeled as 13 failure modes. On the other hand, consider the photographs in Figure 8. These photographs show a crushing mode to be present by the relatively homogeneous bulging and deformation throughout the specimen, whereas the darkened areas localized along inclined planes indicate possible incipience of a shear plane. However, the dominant mode of deformation appears to be a shortening of the longitudinal axis rather than slip along a shear plane. Hence the photographs in Figure 8 are classified as 31 failure modes. Other examples of mixed modes can be seen in the photographs shown in Figures 9-12.

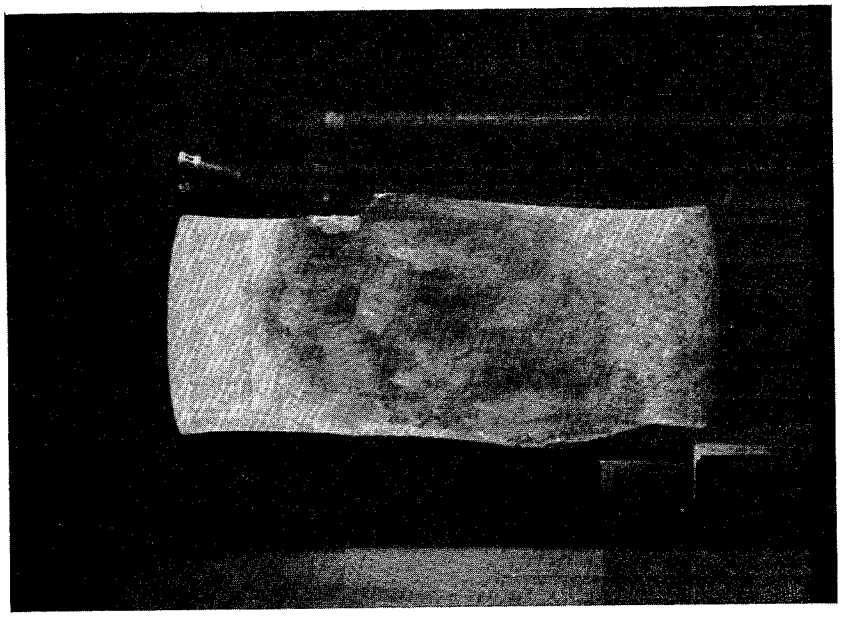

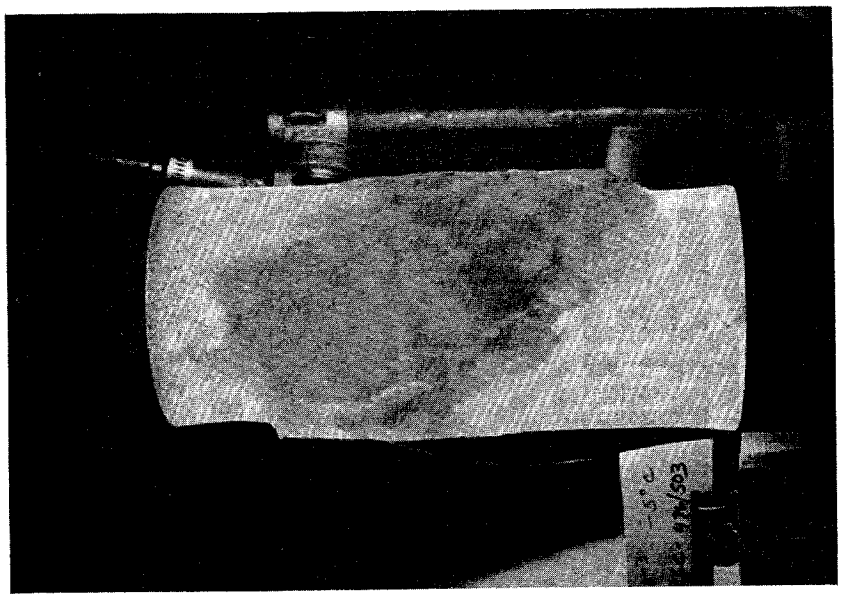

Fig. 7 - Photographic example of the 13 mixed failure mode.

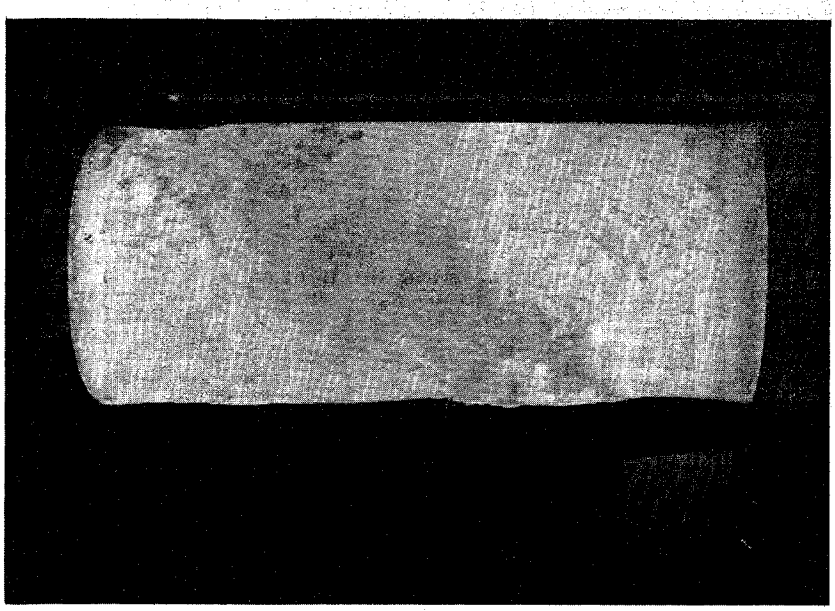

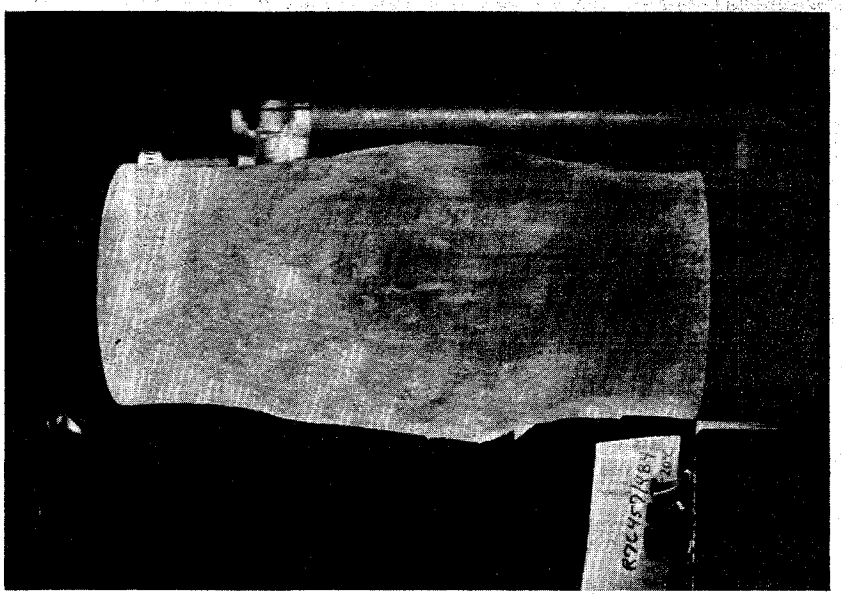

Fig. 8 - Photographic example of the 31 mixed failure mode.

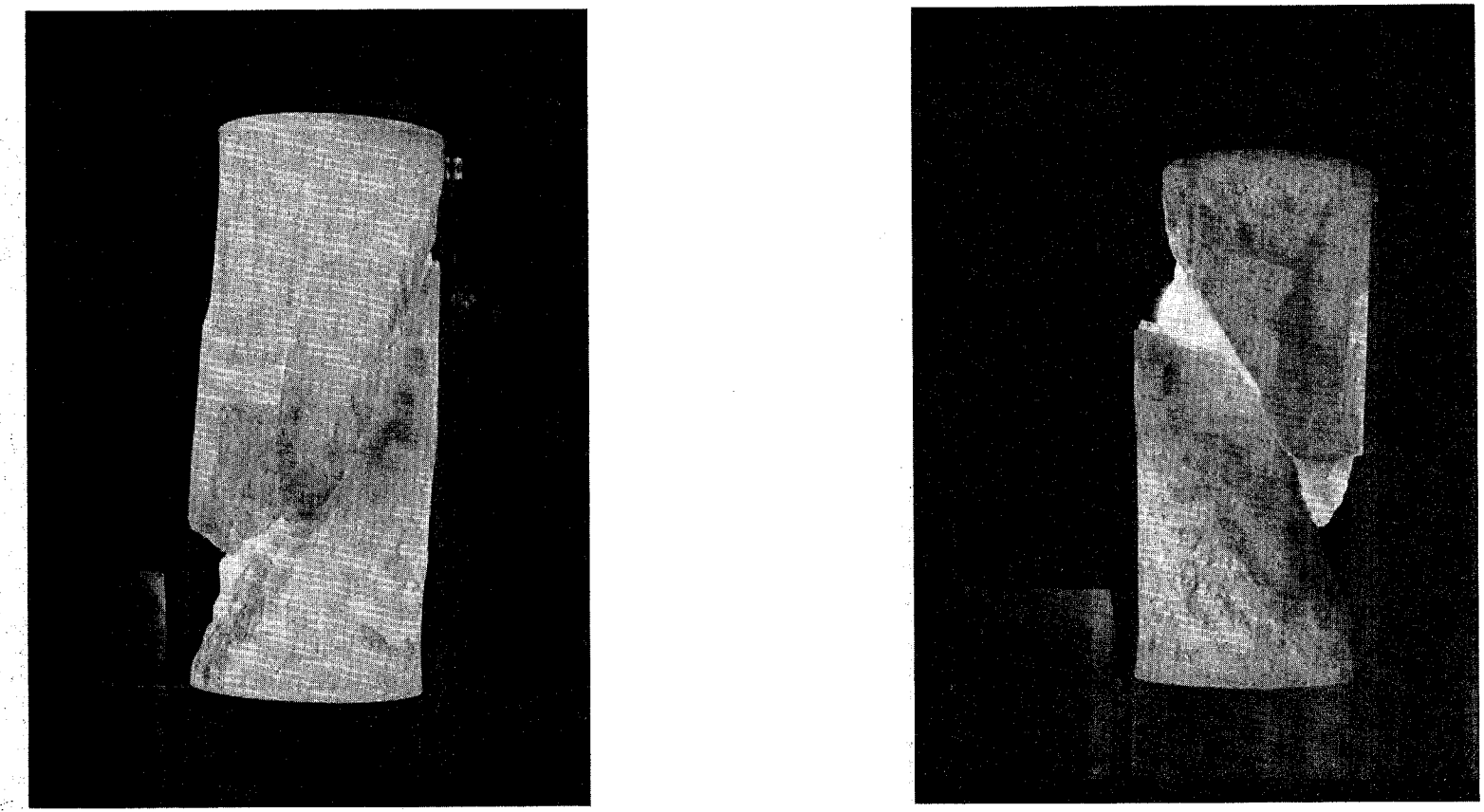

Fig. 9 - Photographic example of the 12 mixed failure mode.

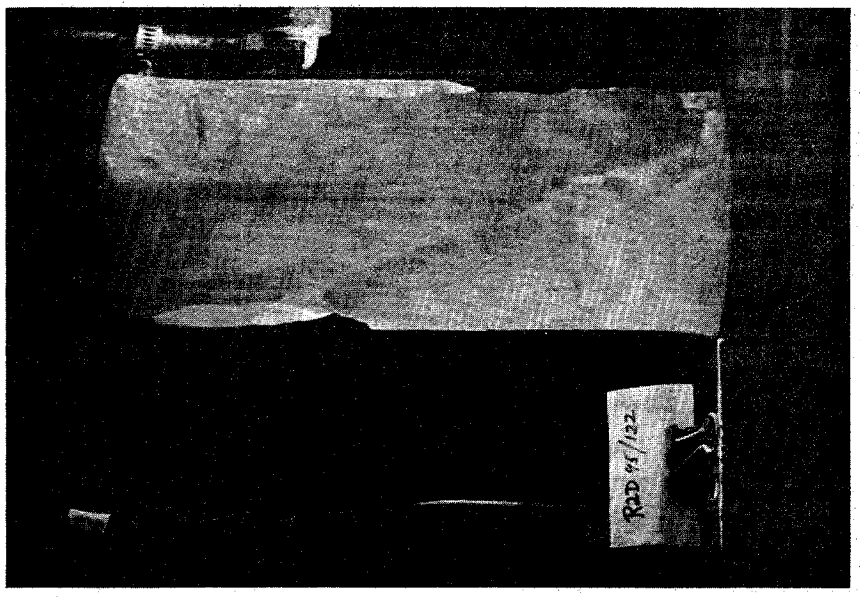

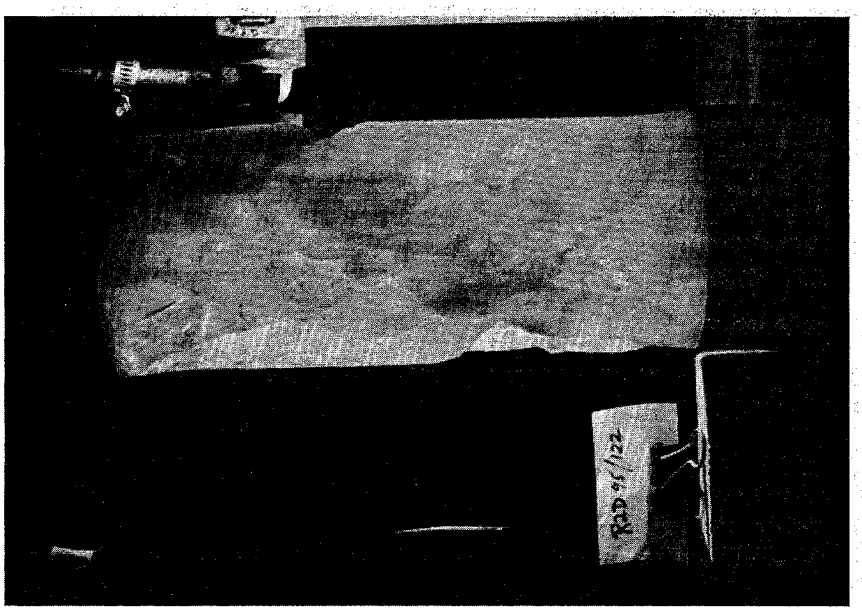

Fig. 10 - Photographic example of the 21 mixed failure mode.

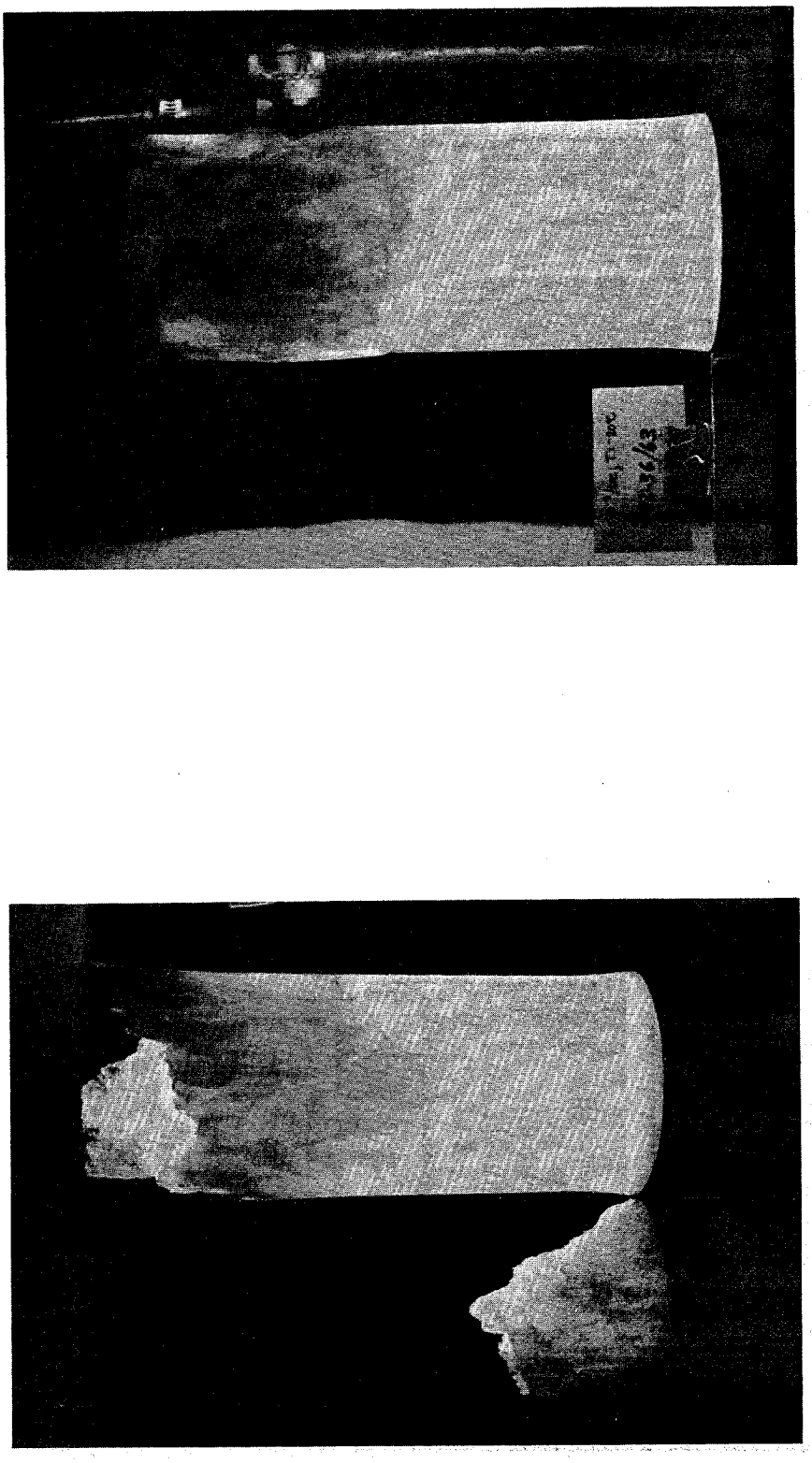

Fig. 11 - Photographic example of the 23 mixed failure mode.

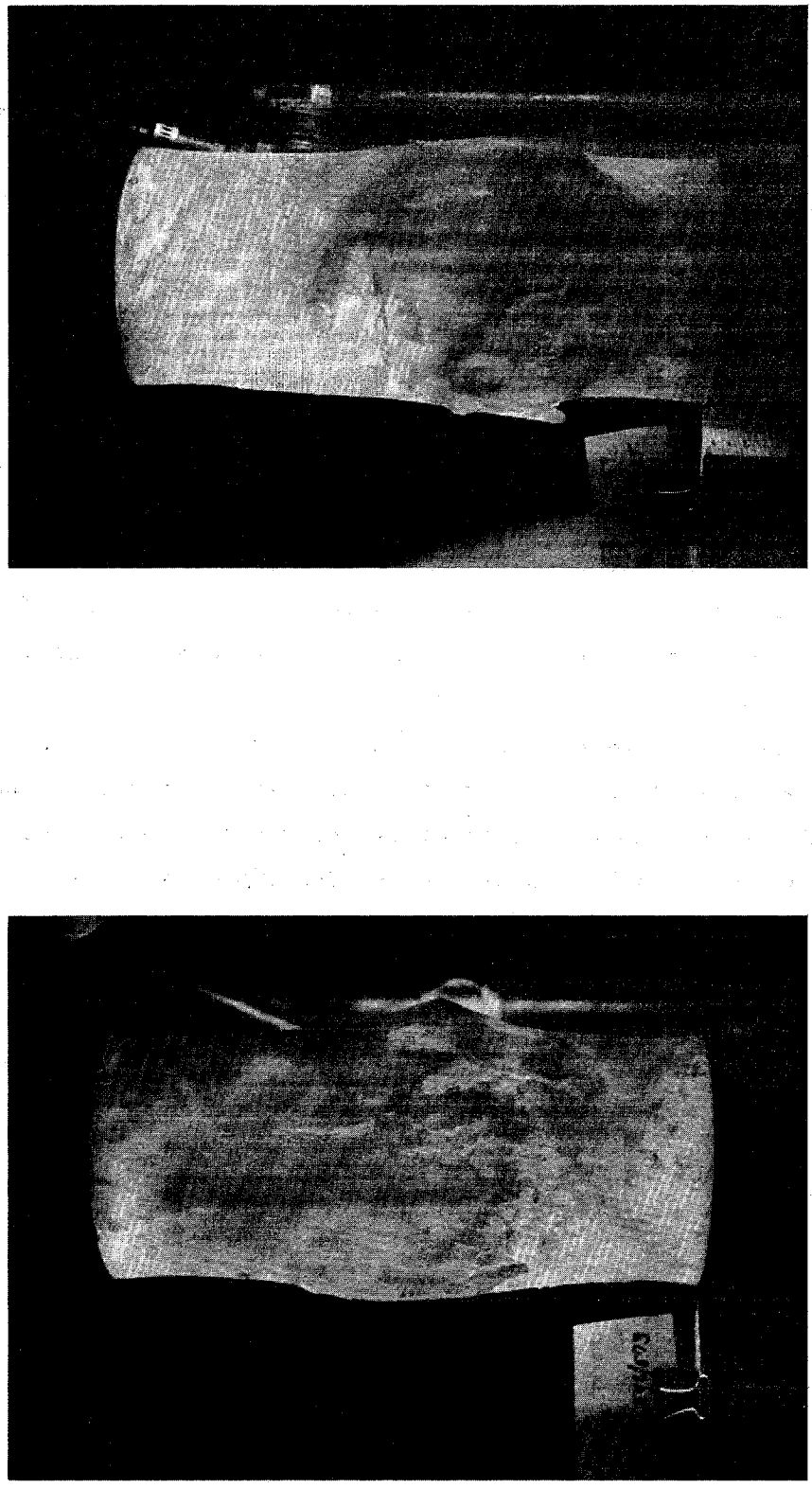

Fig. 12 - Photographic example of the 32 mixed failure mode.

RESULTS

All available photographs were assigned failure modes, and brief comments were recorded for each. The failure mode and comments for each test are listed in Tables 1-4 according to the four test conditions. The frequency of occurrence for each failure mode is given in Table 5.

The assigned failure modes depend greatly on the subjective opinions of the observer. This problem is compounded when several views of the same specimen exist, which, in many cases, give the observer different impressions of the actual failure mode. To investigate the reproducibility of results, the photographs of the specimens tested at $T = -20°C$, $\dot{\varepsilon} = 10^{-5}$/sec were reexamined long after the original failure modes were assigned. Of the 35 original failure modes for the selected test condition, 23 were matched on the second examination. Of the 12 failure modes which did not match the originals, 6 were successful in matching the dominant failure mode and 5 reversed the order of the dominant and secondary failure modes. These results indicate that it is possible to at least identify with some consistency the dominant failure characteristics of each test specimen.

To investigate the effects of temperature and strain rate on the failure modes, we look at the two levels of constant temperature and constant strain rate. Since our experiment to check the reproducibility of results shows the dominant mode can be consistently identified, we list in Table 6 the frequency of occurrence of each fundamental mode acting as the dominant mode. At both levels of constant temperature, we observe the occurrence of the longitudinal splitting mode to increase with increasing strain rate. However, there is no such trend observed for both levels of constant strain rate. At the 10^{-5}/sec strain rate, we observe the crushing mode to increase relative to the other modes as the temperature increases. This trend is not observed for the 10^{-3}/sec strain rate where the occurrence of the crushing mode relative to the other modes is approximately the same for both temperatures.

Due to the subjective nature of assigning failure modes, we would like to have some verification of our observations in Table 6. In our reproducibility experiment, a large source of error was attributed to confusing the dominant and secondary modes. Assuming it is likely that this error is present in all four test conditions, we list in Table 7 the frequency of occurrence of each fundamental mode acting as either the dominant or secondary

Table 1

FAILURE MODES FOR TESTS CONDUCTED
AT $\dot{\varepsilon} = 10^{-3}$/sec, T = -5°C

Test Number	Failure	Comments
R1A-175/201		
R1B-131/157	31	Highly fissured throughout, developing shear plane, some longitudinal cracks.
R2A-110/135	20	Complete rupture into 3 parts, wedge shaped failure surface.
R2B-135/161	23	Complete rupture, highly fissured.
R3A-188/213	31	Highly fissured throughout, shear plane beginning to develop.
R3B-130/155	30	Highly fissured throughout, homogeneous bulging.
R4A-283/309	23	Two longitudinal cracks, beginning to spall, fissured near top.
R4B-299/325	30	Highly fissured throughout, initiation of spalling.
R5A-135/161	23	Complete rupture, crushing mode questionable.
R5B-141/167	23	Complete rupture, wedge shaped failure surfaces, difficult to determine actual failure mode-probably longitudinal cracks with crushing.
R7A-005/031	23	Complete rupture along longitudinal cracks, highly fissured.
R7B-072/098	23	Longitudinal cracks and crushing in lower 2/3, spalling.
R8A-033/059	23	Complete rupture, failure mode not apparent, probably splitting with some crushing.
R8B-011/037	20	Several longitudinal cracks, some spalling.
R2C-049/076	31	Highly fissured, developing shear plane, spalling near top.
R2D-134/161	31	Highly fissured, developing shear plane, beginning to spall.
R4C-244/271	20	Many longitudinal cracks, some spalling.
R4C-309/336	30	Highly fissured, homogeneous bulging, possible shear plane.

Table 1 (continued)

Test Number	Failure	Comments
R4D-228/255	20	Fracture along brine channels, wedge shape rupture.
R7C-007/034	23	Splitting along initial fracture, localized fissures.
R6A-398/425	32	Large bulge near center with longitudinal cracks, beginning to spall.
R6A-504/531	30	Highly fissured, homogeneous bulging.
R7D-088/114	30	Homogeneous bulging, beginning to spall.
R9C-080/107	31	Highly fissured in lower 2/3 of sample, initiation of shear plane.
R9D-082/109	10	Shear plane at approximately 45°.
R1A-300/326	20	Complete rupture, difficult to determine failure mode, wedge shaped failure surfaces.
R1B-216/241	13	Shear plane at 45°, much crushing above and below shear plane.
R1B-243/268	32	Uniform bulging, longitudinal cracks and spalling are initiating.
R2A-285/310	32	Deformed throughout specimen, some spalling, no clear failure surface.
R2A-383/408	20	Spalling, minor local crushing.
R2B-351/377	12	Highly deformed shear plane surrounded by longitudinal cracks.
R2B-438/464	30	Highly fissured around a localized crushing zone, complete rupture.
R3A-348/373	20	Complete wedge shaped rupture, some localized crushing.
R3A-401/427	13	Shear plane at 40°, crushing above shear plane.
R3B-239/265	30	Highly fissured throughout, homogeneous bulging, shear plane beginning to form.
R3B-331/357	32	Highly fissured throughout, longitudinal cracks beginning to form.

Table 1 (continued)

Test Number	Failure	Comments
R4A-398/423	30	Highly fissured throughout, localized bulging, possible shear plane beginning to form.
R4B-358/384	32	Crushing in top 2/3, some longitudinal cracks and spalling.
R4B-420/446	10	Complete rupture, little evidence of deformation outside of shear plane.
R5A-473/499	13	Predominantly shear plane, some localized crushing.
R5B-287/313	20	Complete rupture, wedge shaped failure surface.
R5B-370/396	31	Predominantly crushing, shear plane beginning to form.
R7A-232/258	30	Highly fissured throughout, nonhomogeneous bulging near the top.
R7A-295/321	20	Two major longitudinal cracks, one large area of spalling.
R7B-175/201	10	Shear plane at 50°, no apparent deformation outside of shear plane.
R7B-440/466	23	Some spalling and localized crushing.
R8A-305/331	30	Homogeneous bulging, highly fissured throughout.
R8A-384/410	10	Complete rupture along shear plane.
R8B-300-326	30	Uniform bulging, highly fissured throughout.
R8B-483/509	23	Deformation localized in top 1/2, complete rupture.
R2C-196/223	31	Crushing mode followed by formation of shear plane.
R2C-278/305	31	Predominantly crushing, shear plane beginning to form.
R2D-220/347	12	Predominantly shear plane, major longitudinal cracks, some spalling.
R2D-334/371	13	45° shear plane, extensive crushing.
R4C-414/441	30	Homogeneous bulging.

Table 1 (continued)

Test Number	Failure	Comments
R4C-512/539	10	One clear shear plane 60° with respect to horizontal, some crushing.
R4D-495/522	20	Initially many brine channels at 70°-80° WRT horizontal, much fracturing along brine channels, complete rupture.
R6C-476/503	13	Difficult to determine dominant mode.
R7C-143/170	30	Highly fissured throughout, possible shear plane beginning to form.
R7C-541/568	30	Homogeneous bulging, fissured throughout.
R7D-223/250	30	Homogeneous bulging, fissured throughout.
R7D-312/339	30	Bulging localized but symmetric near top, deformation localized near top half.
R9A-445/482	13	45° shear plane, much crushing.
R9B-329/356	20	Complete rupture, wedge shaped failure surface.
R9C-332/359	30	Symmetric bulging localized near top, bottom 1/3 relatively undeformed.
R5D-249/276	13	45° shear plane near bottom, crushing above shear plane.
R10A-269/296	13	Difficult to determine dominant mode.
R10B-274/301		
R10C-445/472	21	Many longitudinal cracks, shear plane beginning to form, some spalling.
R10D-231/258	31	Deformation restricted to top 1/3, some longitudinal cracks.

Table 2

FAILURE MODES FOR TESTS CONDUCTED AT $\dot{\varepsilon} = 10^{-3}$/sec, T = -20°C

Test Number	Failure	Comments
R1C-127/154		
R1D-153/178	23	Complete rupture, highly fissured around failure surface.
R2C-129/156	23	Some Spalling, complete rupture along single failure.
R2D-095/122	21	Spalling, appearance of shear plane, possible wedge shape failure surface forming.
R4D-198/225	20	Single failure surface along brine channels, spalling.
R6A-531/558	30	Homogeneous bulging.
R6C-134/161	12	Shear plane with longitudinal cracks, some spalling.
R7C-092/119	23	Spalling, localized deformation near top.
R7D-036/063	23	Crushing near top, some spalling, numerous longitudinal cracks.
R9A-071/098	12	Shear plane with longitudinal cracks, some crushing.
R9B-076/103	13	Complete rupture along a shear plane, highly fissured throughout.
R9C-049/076	31	Homogeneous bulging, highly fissured throughout, shear plane beginning to form.
R9D-150/177	31	Localized bulging, highly fissured near top, shear plane.
R10A-238/265	23	Complete rupture, wedge shaped failure surface, some crushing.
R10B-084/111	31	Deformed throughout, shear plane beginning to form, appearance of some longitudinal cracks.
R1C-349/375	20	Complete rupture, almost wedge shaped failure surface, presence of crushing uncertain.
R1C-384/410	20	Predominantly longitudinal cracks, some localized crushing, minor spalling.

Table 2 (continued)

Test Number	Failure	Comments
R1D-179/206	20	Predominantly longitudinal cracks, some localized crushing, minor spalling.
R1D-285/312	20	Complete rupture, wedge shaped failure surface.
R2C-226/253	13	Highly localized deformation along shear plane, some longitudinal cracks.
R2C-310/337	32	Highly deformed in top 2/3, many longitudinal cracks.
R2D-265/292	10	Well deformed shear plane at 65° WRT horizontal.
R2D-406/433	31	Highly fissured in top 2/3, shear plane beginning to develop.
R4C-482/509	30	Homogeneous bulging.
R4C-543/570	31	Highly deformed in bottom 1/2, shear plane beginning to develop.
R4D-382/409	31	Highly fissured throughout, shear plane beginning to develop.
R4D-414/441	12	Shear plane with several longitudinal cracks.
R4D-525/552	10	Shear plane in top half, minor crushing along shear plane, some spalling.
R6C-559/586	30	Homogeneous bulging, highly fissured throughout.
R7C-457/484	31	Highly fissured throughout sample, shear plane developing.
R7C-572/599	20	Complete rupture, wedge shape failure surface, presence of crushing cannot be determined.
R7D-254/281	31	Complete rupture along shear plane, highly fissured.
R7D-546/573	32	Predominantly crushing of center section with several longitudinal cracks.
R9A-424/451	12	Shear plane with longitudinal cracks, some spalling, sample relatively undistorted.
R9B-417/444	12	Shear plane with some localized crushing, longitudinal cracks present, some spalling, sample relatively undistorted.

Table 2 (continued)

Test Number	Failure	Comments
R9C-507/534	30	Homogeneous bulging, fissured throughout.
R9D-348/375	20	Predominantly longitudinal cracks, wedge shaped failure surface beginning to appear.
R10A-407/434	30	Bulging of top 2/3 of sample, lower 1/2 undeformed.
R10B-449/476	30	Homogeneous bulging, deformed (fissured) throughout.
R10C-506/533	31	Localized bulging of bottom 1/2, shear plane developing.
R10D-508/535	30	Localized bulging of bottom 1/2.

Table 3

FAILURE MODES FOR TESTS CONDUCTED
AT $\dot{\varepsilon} = 10^{-5}$/sec, T = -5°C

Test Number	Failure	Comments
R1A-062/089	31	Localized bulging in lower 1/2, shear plane beginning to develop, highly fissured in lower 1/2.
R1B-062/089	31	Localized bulging in top 1/2, shear plane beginning to develop, highly fissured in top half.
R2A-140/165	30	Homogeneous bulging, highly fissured throughout.
R2B-094/121	10	Well-defined shear plane, little deformation outside shear plane.
R3A-106/131	30	Homogeneous bulging, highly fissured throughout.
R3B-161/187	13	Shear plane at 30° WRT horizontal, undeformed in top half, highly fissured in lower 1/2, bulging in lower 1/2.
R4A-312/338	30	Right side uniform bulge, left side localized bulge, possible initiation of shear plane, highly fissured throughout.
R4B-328/354	31	Left side uniform bulge, right side localized bulge, definite shear plane initiation, highly fissured in top 2/3.
R5A-165/191	13	Shear plane across diagonal of specimen, localized crushing bulge at either end of shear plane.
R5B-075/101	30	Deformation mainly in top 1/2, areas of highly localized deformation, possible cup and cone failure surfaces developing.
R7A-059/085	30	Uniform bulging of top 1/2, highly fissured in top 1/2.
R7B-126/152	10	Deformation mainly restricted to shear plane, sample relatively undeformed except for bulges at shear plane.
R8A-133/159	13	Shear plane at 45°, some crushing in top 1/2.
R8B-162/189	30	Localized bulging in top and bottom half.

Table 3 (continued)

Test Number	Failure	Comments
R3C-095/122	30	Localized bulging in top half, highly fissured in top half.
R3D-159/186	30	Localized bulging in top 1/2.
R5C-039/066	30	Localized bulging in bottom 1/2, highly fissured in bottom 1/2.
R5D-159/186	30	Localized bulging in bottom 1/2, highly fissured in bottom 1/2.
R6C-166/193	10	Shear plane at 30° WRT horizontal, some crushing in lower 1/2.
R8C-048/075	31	Crushing in lower 1/2, shear plane beginning to develop, bulging in lower half.
R8D-236/263	30	Highly deformed in top 1/3, large bulge and highly fissured in top 1/3.
R10C-063/090	30	Fissured throughout, relatively homogeneous bulging, possibly shear plane beginning to form.
R10D-126/153	30	Deformation localized in top 1/2.
R1A-226/252	31	Crushing in top 1/2, shear plane beginning to form.
R1A-399/425	13	Shear plane in top 1/2, crushing below shear plane.
R1B-320/346	32	Localized bulging at top right and lower left, barrel bulging top left, some longitudinal cracks.
R1B-429/455	31	Crushing of lower 1/2, shear plane beginning to form.
R2A-205/230		
R2A-314/339	12	Shear plane developing along brine channels, longitudinal cracks along brine channels.
R2B-408/434	13	Shear plane at 45° in lower 1/3, localized crushing just above shear plane.
R2B-468/494	31	Shear plane developing, much crushing above apparent shear plane, relatively little crushing below apparent shear plane.

Table 3 (continued)

Test Number	Failure	Comments
R3A-220/245	31	Deformation localized in top 1/2, possible double shear plane forming.
R3A-430/456	31	Deformed throughout, shear plane beginning to develop.
R3B-363/389	30	Crushing of lower 1/2.
R4A-426/452	32	Deformed throughout, little bulging, longitudinal cracks beginning to initiate.
R4B-391/417	31	Definite shear plane, much crushing and some bulging below shear plane,
R4B-449/475	13	Lower 1/3 undeformed, some crushing above shear plane.
R5A-397/423	10	Shear plane in lower 1/3, deformation localized along shear plane.
R5A-442/468	30	Homogeneous bulging, fissures throughout sample.
R5A-504/530	30	Bulging and fissures localized in lower 1/2.
R5B-341/367	31	Highly fissured throughout specimen, shear plane beginning to develop.
R5B-398/423	13	Parallel, double shear plane, crushing above top shear plane, deformation localized in lower 1/2.
R7A-263/289	31	Uniform crushing with development of shear plane.
R7A-342/368	32	Localized crushing in top 1/3, some longitudinal cracks.
R7B-241/267	30	Crushing of top 1/2, highly fissured in top 1/2.
R7B-410/436	10	Complete rupture along brine channels, no apparent crushing outside of shear plane (i.e., failure surface).
R8A-164/190	10	Highly deformed along shear plane.
R8A-432/458	13	Shear plane at 65°, crushing above shear plane, relatively undeformed below shear plane.
R8B-333/359	30	Relatively homogeneous bulging, possible initiation of shear plane.

Table 3 (continued)

Test Number	Failure	Comments
R8B-515/541	30	Crushing of top 1/2, uniform bulging of top 1/2.
R3C-296/323	30	Uniform deformation in top 1/2, bottom 1/2 undeformed.
R3C-380/407	10	Distinct shear plane 60° WRT horizontal, some spalling.
R3D-219/246	30	Deformation in top 1/2 only, possible shear plane initiation.
R3D-287/314	30	Homogeneous bulging.
R5C-219/246	30	Deformation and bulging in lower 1/2, shear lip developing.
R5C-282/309	31	Deformation mainly in top 1/2, shear plane developing.
R5D-225/252	30	Uniform deformation and bulging throughout.
R5D-294/321	31	Uniform bulging, highly deformed along a developing shear plane.
R6A-562/589	30	Uniform bulging of top 2/3, possible shear plane developing.
R6C-529/556	30	Uniform bulging and deformation.
R8C-378/405	13	Deformation localized along shear plane, uniform bulging.
R8C-476/503	10	Definite shear plane along brine channels.
R8D-446/473	10	Shear plane at 65° WRT horizontal, some localized crushing.
R8D-534/561	30	Deformation mainly in top 1/2, possible shear plane developing, nonuniform bulging of top 1/2.
R9A-341/368	30	Deformation mainly in top 1/2, possible shear plane developing.
R9B-385/412	30	Uniform deformation, possible shear plane developing.
R9C-426/453	30	Deformation mainly in lower 1/2, uniform bulging of lower 1/2.

Table 3 (continued)

Test Number	Failure	Comments
R9D-181/208	13	Shear plane at 45° in top 1/3, some crushing below shear plane probably due to end cap constraint, deformation localized in top 1/3.
R10A-351/378	30	Uniform bulging, possible shear plane initiation.
R10B-351/378	10	Shear plane at 45° in top 1/2.
R10C-316/343	30	Uniform bulging of lower 1/2, possible shear plane initiation.
R10D-325/352	31	Deformation localized in top 1/2, shear plane beginning to form.

Table 4

FAILURE MODES FOR TESTS CONDUCTED
AT $\dot{\varepsilon} = 10^{-5}$/sec, T = -20°C

Test Number	Failure	Comments
R1C-065/092		
R1D-071/098	10	Shear plane at 45° in top 1/2, some cracking along initial flaws.
R3C-128/155	31	Deformation in top 2/3, shear plane initiating.
R3D-129/156	31	Shear plane at 30° WRT horizontal, deformation in top 1/2, horizontal crack near bottom.
R5C-097/124		
R5D-121/148	13	Deformation mainly in lower 1/2 with much fissuring, top half relatively undeformed.
R6A-461/488	31	Uniform bulging with shear plane beginning to form in middle section, highly fissured in test section.
R8C-165/192	13	Highly fissured above shear plane, undeformed below shear plane.
R8D-192/219	13	Shear plane formed in lower 1/3 along initial flaw, highly fissured below shear plane, relatively undeformed above shear plane with 2 longitudinal cracks.
R9A-125/152	13	Highly fissured in top 1/2 with shear plane, lower 1/2 undeformed.
R9B-043/070	31	Deformation in top 2/3, shear plane developing in top 2/3.
R10A-195/222	30	Uniform bulging, possible shear plane near top.
R10B-243/270	13	Shear plane at 65° WRT horizontal, highly deformed above shear plane, undeformed below shear plane.
R10C-032/059	13	Shear plane at 45°, undeformed above shear plane, deformed below shear plane.
R10D-157/184	30	Mainly deformed in lower half, some deformation in upper half.
R1C-210/236	13	Shear plane at 45°, highly fissured throughout specimen.

Table 4 (continued)

Test Number	Failure	Comments
R1C-240/266		
R1D-209/236	12	Shear plane in top 1/3, highly fissured in top 2/3, longitudinal cracks appearing.
R1D-315/342	31	Extensive bulging and fissuring in lower 2/3, shear plane beginning to develop.
R3C-329/359	10	Deformation mainly restricted to shear plane, shear plane at 45° in top 1/2.
R3C-411/438	13	Shear plane across entire sample and along brine channels, some bulging in lower half.
R3D-250/277	30	Bulging mainly in top 1/2, possible shear plane beginning to develop.
R3D-318/345	30	Uniform bulging, highly fissured throughout sample.
R5C-250/277	32	Deformation in lower 1/2, some spalling and longitudinal cracks, possible wedge shape failure surface beginning to form.
R5C-328/355		
R5D-255/282		
R5D-325/352		
R6A-661/688	13	Complete rupture along shear plane, some crushing outside shear plane.
R6C-589/616	30	Uniform bulging, deformed throughout specimen.
R8C-444/471	12	Rupture along 60° shear plane, some spalling and longitudinal cracks.
R8C-508/535	31	Crushing in top 2/3, shear plane beginning to form.
R8D-477/504	12	Rupture along 65° shear plane, some longitudinal cracks.
R8D-565/592	30	Mainly crushing in lower half, uniform bulge on one side and bulge in lower half on opposite side.
R9A-523/550	13	45° shear plane in lower half, some crushing outside of shear plane in upper half.

Table 4 (continued)

Test Number	Failure	Comments
R9B-449/476	31	Highly fissured in middle, cup and cone failure surfaces beginning to form.
RC-395/422	30	Highly deformed in top half, uniform bulging of top half.
R9D-317/344	30	Uniform bulging of entire sample, deformation mainly in lower 2/3.
R10A-320/347	13	Wide shear plane in lower half, little crushing outside shear plane.
R10B-418/445	30	Uniform bulging of top 2/3, deformation mainly in top 2/3.
R10C-347/374	13	50° shear plane, deformation mainly in shear plane.
R10D-356/383	30	Crushing of lower 1/2.

Table 5

FREQUENCY OF OCCURRENCE FOR EACH MIXED FAILURE MODE

Test Conditions	Failure Modes								
	10	12	13	20	21	23	30	31	32
$\dot{\varepsilon} = 10^{-3}$/sec, T = -5°C	5	2	8	11	1	10	17	9	5
$\dot{\varepsilon} = 10^{-3}$/sec, T = -20°C	2	5	2	7	1	4	6	9	2
$\dot{\varepsilon} = 10^{-5}$/sec, T = -5°C	10	1	10	0	0	0	32	15	3
$\dot{\varepsilon} = 10^{-5}$/sec, T = -20°C	2	4	12	0	0	0	10	7	1

Table 6

FREQUENCY OF OCCURRENCE FOR EACH FUNDAMENTAL MODE ACTING AS THE DOMINANT MODE

	FUNDAMENTAL FAILURE MODES					
	1	2	3	1	2	3
10^{-5}/sec	36	4	60	25	5	30
10^{-3}/sec	25	29	49	19	19	23
$\dot{\varepsilon}$ / T	−5 °C			−20 °C		

Table 7

FREQUENCY OF OCCURRENCE FOR EACH FUNDAMENTAL MODE ACTING AS EITHER THE DOMINANT OR THE SECONDARY MODE

	FUNDAMENTAL FAILURE MODES					
	1	2	3	1	2	3
10^{-5}/sec	21	0	50	18	0	18
10^{-3}/sec	15	22	31	9	12	17
$\dot{\varepsilon}$ / T	−5 °C			−20 °C		

failure mode. This procedure will increase the possibility that the actual dominant mode will appear in the frequency count. In Table 7, we again observe that the occurrence of the longitudinal splitting mode increases with increasing strain rate for both levels of constant temperature. Table 7 also shows that the occurrence of the crushing mode relative to the other modes increases with increasing temperature for both levels of constant strain rate in contrast to Table 6, which shows this trend for only one level of constant strain rate.

DISCUSSION

Both Tables 6 and 7 show that increasing strain rate affects the failure mode by increasing the occurrence of the longitudinal splitting mode. This observation is consistent with the concept of linear fracture mechanics which requires a state of elasticity in the vicinity of a crack tip as a condition for crack propagation. At high strain rates this condition is satisfied. At lower strain rates there will be a considerable amount of ductile flow at the tips of any existing microcracks which would hinder their propagation. As a consequence, large numbers of microcracks would nucleate and arrest throughout the specimen rather than a few propagating along the length in an unstable manner.

The effect of temperature on the failure mode is not as easily explained as the strain rate effect, but Tables 6 and 7 do suggest that increasing temperature favors the occurrence of the crushing mode. Although it is impossible to make any definitive statements about why this observation could, in general, be true, an explanation can at least be hypothesized.

Rather than think of the shear and crushing modes as distinct failure modes, it is perhaps better to think of them as different stages of a single failure process. In most geological materials such as ice, microcracking is one of the fundamental micromechanical processes which controls the deformation of the material. The material is usually tested by loading a specimen with a homogeneous state of stress such as uniaxial compression. The material will initially respond by nucleating microcracks whose spatial distribution is fairly uniform throughout the specimen. The resulting deformation is homogeneous and is associated with the crushing mode. However, if during the loading process certain conditions are satisfied, the microcracks

can begin to coalesce in certain planes. The resulting deformation becomes localized along those planes which is a characteristic of the shear mode.

The appearance of shear planes should be viewed as a material instability. If a constitutive law were available for ice, then it would be possible to actually calculate the conditions (i.e., state of stress) necessary for the localization of deformation to occur. In fact, this has been done for metals using various plasticity laws to predict the onset of necking in tensile specimens. In our case, the conditions for localization would define the bifurcation point between the crushing and shear modes and would depend on the material parameters of the appropriate constitutive law. For ice, we can hypothesize that the lower strengths associated with high temperatures do not satisfy the conditions necessary for the incipience of shear planes.

Our observations regarding the effects of temperature and strain rate on the failure mode were obtained from two different levels of constant temperature and strain rate and are supported by the fact that these observations hold up under two methods (i.e., Tables 6 and 7) of counting the frequency of occurrence. However, no firm conclusions should be made without taking into account the physical properties of the test specimens. The crystallographic structure of the specimen is probably the most important of all physical properties. It would be reasonable to expect, for example, that a columnar specimen would have different failure characteristics than a granular specimen. If strong correlations between failure modes and crystal structure are found and a particular ice type dominates a given test condition, then some doubts would be raised as to the general validity of our observed temperature and strain rate effects. Work has begun to define the crystallographic structure of all available test specimens. Upon the completion of that work, the correlations between crystal structure and failure mode can be investigated.

SUMMARY AND CONCLUSION

Three fundamental failure modes are defined to describe the failure of the Phase I uniaxial compression tests. These fundamental modes are shear, longitudinal splitting, and crushing. Inspection of the available photographs of the tested specimen shows that the failure usually consists of more than one fundamental mode. As a result, a mixed mode classification system is

devised. This system identifies a dominant and a secondary failure mode. All available photographs are inspected and assigned failure modes according to this mixed mode classification scheme. Brief comments describing the failure mode are also recorded for each specimen.

The effects of temperature and strain rate on the failure mode are investigated. Results of this investigation show that the occurrence of the longitudinal splitting mode increases with increasing strain rate, and the occurrence of the crushing mode increases with increasing temperature. These results should not be considered final until the effects of physical properties on the failure mode are investigated. However, they do illustrate a dependence of failure mode on temperature and strain rate which should be kept in mind when postulating a failure mode for a particular ice loading scenario.